

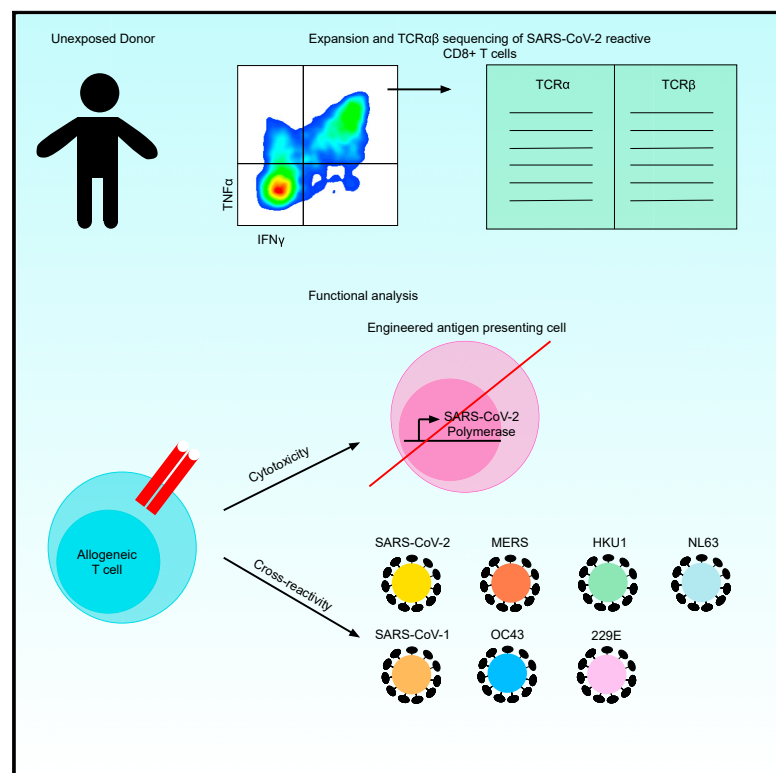


Since January 2020 Elsevier has created a COVID-19 resource centre with free information in English and Mandarin on the novel coronavirus COVID-19. The COVID-19 resource centre is hosted on Elsevier Connect, the company's public news and information website.

Elsevier hereby grants permission to make all its COVID-19-related research that is available on the COVID-19 resource centre - including this research content - immediately available in PubMed Central and other publicly funded repositories, such as the WHO COVID database with rights for unrestricted research re-use and analyses in any form or by any means with acknowledgement of the original source. These permissions are granted for free by Elsevier for as long as the COVID-19 resource centre remains active.

# HLA-A\*02:01 restricted T cell receptors against the highly conserved SARS-CoV-2 polymerase cross-react with human coronaviruses

## Graphical abstract



## Authors

Pavlo A. Nesterenko, Jami McLaughlin, Brandon L. Tsai, ..., James R. Heath, Paul C. Boutros, Owen N. Witte

## Correspondence

owenwitte@mednet.ucla.edu

## In brief

Nesterenko et al. identify T cell responses with potential to confer long-term immunity against SARS-CoV-2. The machinery responsible for replicating the viral genome is highly conserved and, as shown by Nesterenko et al., can be effectively targeted by CD8<sup>+</sup> T cells.

## Highlights

- The RNA-dependent RNA-polymerase is highly conserved among human coronaviruses
- CD8<sup>+</sup> T cells from unexposed donors recognize SARS-CoV-2 polymerase epitopes
- TCR engineered T cells kill target cell lines that express the polymerase
- Polymerase-reactive TCRs cross-react with seasonal coronaviruses



## Report

# HLA-A\*02:01 restricted T cell receptors against the highly conserved SARS-CoV-2 polymerase cross-react with human coronaviruses

Pavlo A. Nesterenko,<sup>1</sup> Jami McLaughlin,<sup>2</sup> Brandon L. Tsai,<sup>3,4,5,6,7</sup> Giselle Burton Sojo,<sup>2</sup> Donghui Cheng,<sup>7</sup> Daniel Zhao,<sup>3,4,5,6,7</sup> Zhiyuan Mao,<sup>8</sup> Nathanael J. Bangayan,<sup>8</sup> Matthew B. Obusan,<sup>2</sup> Yapeng Su,<sup>9</sup> Rachel H. Ng,<sup>9,10</sup> William Chour,<sup>9,11,12</sup> Jingyi Xie,<sup>9,10</sup> Yan-Ruide Li,<sup>2</sup> Derek Lee,<sup>2</sup> Miyako Noguchi,<sup>2</sup> Camille Carmona,<sup>13</sup> John W. Phillips,<sup>2</sup> Jocelyn T. Kim,<sup>13</sup> Lili Yang,<sup>1,2,6,7</sup> James R. Heath,<sup>9,14</sup> Paul C. Boutros,<sup>3,4,5,6,7,8</sup> and Owen N. Witte<sup>1,2,6,7,8,14,15,\*</sup>

<sup>1</sup>Molecular Biology Institute, University of California, Los Angeles, Los Angeles, CA 90095, USA

<sup>2</sup>Department of Microbiology, Immunology, and Molecular Genetics, University of California, Los Angeles, Los Angeles, CA 90095, USA

<sup>3</sup>Department of Human Genetics, University of California, Los Angeles, Los Angeles, CA 90095, USA

<sup>4</sup>Department of Urology, University of California, Los Angeles, Los Angeles, CA 90095, USA

<sup>5</sup>Institute for Precision Health, University of California, Los Angeles, Los Angeles, CA 90095, USA

<sup>6</sup>Jonsson Comprehensive Cancer Center, University of California, Los Angeles, Los Angeles, CA 90095, USA

<sup>7</sup>Eli and Edythe Broad Center of Regenerative Medicine and Stem Cell Research, University of California, Los Angeles, Los Angeles, CA 90095, USA

<sup>8</sup>Department of Molecular and Medical Pharmacology, University of California, Los Angeles, Los Angeles, CA 90095, USA

<sup>9</sup>Institute for Systems Biology, Seattle, WA 98109, USA

<sup>10</sup>Department of Bioengineering, University of Washington, Seattle, WA 98105, USA

<sup>11</sup>Division of Biology and Biological Engineering, California Institute of Technology, Pasadena, CA 91125, USA

<sup>12</sup>Keck School of Medicine, University of Southern California, Los Angeles, CA 90033, USA

<sup>13</sup>Division of Infectious Diseases, Department of Medicine, University of California, Los Angeles, Los Angeles, CA 90095, USA

<sup>14</sup>Parker Institute for Cancer Immunotherapy, University of California, Los Angeles, Los Angeles, CA 90095, USA

<sup>15</sup>Lead contact

\*Correspondence: [owenwitte@mednet.ucla.edu](mailto:owenwitte@mednet.ucla.edu)

<https://doi.org/10.1016/j.celrep.2021.110167>

## SUMMARY

Cross-reactivity and direct killing of target cells remain underexplored for severe acute respiratory syndrome coronavirus-2 (SARS-CoV-2)-specific CD8<sup>+</sup> T cells. Isolation of T cell receptors (TCRs) and overexpression in allogeneic cells allows for extensive T cell reactivity profiling. We identify SARS-CoV-2 RNA-dependent RNA polymerase (RdRp/NSP12) as highly conserved, likely due to its critical role in the virus life cycle. We perform single-cell TCR $\alpha\beta$  sequencing in human leukocyte antigen (HLA)-A\*02:01-restricted, RdRp-specific T cells from SARS-CoV-2-unexposed individuals. Human T cells expressing these TCR $\alpha\beta$  constructs kill target cell lines engineered to express full-length RdRp. Three TCR constructs recognize homologous epitopes from common cold coronaviruses, indicating CD8<sup>+</sup> T cells can recognize evolutionarily diverse coronaviruses. Analysis of individual TCR clones may help define vaccine epitopes that can induce long-term immunity against SARS-CoV-2 and other coronaviruses.

## INTRODUCTION

Over 4 million people have died from coronavirus disease 2019 (COVID-19) as of August 2021 (World Health Organization). Many individuals are now immune as a result of successful vaccination campaigns and protection afforded by natural infection with severe acute respiratory syndrome coronavirus-2 (SARS-CoV-2) (Anand et al., 2021; Baden et al., 2021; Lumley et al., 2020; Polack et al., 2020; Sadoff et al., 2021). The virus continues to evolve and may escape immune responses generated against the original sequence (Harvey et al., 2021; Planas et al., 2021). The BNT162b2 mRNA vaccine is 88% effective against the new Delta variant compared with 93.7% for the alpha variant

that was circulating previously (Bernal et al., 2021). Increased spread in vaccinated populations necessitates further understanding of the SARS-CoV-2 immune response.

This pandemic can only be controlled by herd immunity against contemporary strains of the virus. Vaccination against the wild-type spike protein can prevent COVID-19 (Baden et al., 2021; Polack et al., 2020; Sadoff et al., 2021). SARS-CoV-2 vaccines target the spike protein by generating neutralizing antibodies that prevent host cell infection (Khoury et al., 2021; Lumley et al., 2020). SARS-CoV-2 variants often contain multiple mutations in the spike protein and can resist antibody neutralization, creating the possibility that, upon further diversification, viral variants may escape current vaccine defenses



(Hoffmann et al., 2021; Kuzmina et al., 2021; Muik et al., 2021; Planas et al., 2021; Wang et al., 2021). Cytotoxic T cells kill infected cells, thereby directly limiting viral dissemination once the infection occurs (Hall et al., 1986; Harty et al., 2000; Jozwik et al., 2015; McMichael et al., 1983). T cell recognition is not limited to surface proteins like the spike protein; more conserved proteins can be targeted. Internal SARS-CoV-2 proteins are more conserved than the spike and may present a therapeutic opportunity for generating T cell responses that can recognize many coronavirus strains (Grifoni et al., 2020a). T cell vaccine strategies, targeting the nucleocapsid protein, are being explored to generate long-term immunity against SARS-CoV-2 (Dutta et al., 2020; Gauttier et al., 2020; Sieling et al., 2021). It remains unknown which epitopes elicit the most effective antiviral responses (Chen and John Wherry, 2020).

Initial evidence for T cell control of respiratory infections was provided by children with genetic defects in T cell development (Hall et al., 1986). Resident memory T cells, which are permanently localized in non-lymphoid tissues, including the lung, are thought to mediate antiviral responses (Jozwik et al., 2015). In a human respiratory syncytial virus (RSV) infection, disease severity was inversely correlated with the preexisting T cells in the lung (Jozwik et al., 2015). Adoptive transfer of highly functional T cell clones can reduce severity of viral diseases as well (Einsele et al., 2002; Feuchtinger et al., 2010a). The mechanism of respiratory viral infection T cell control is thought to happen through Fas and perforin-mediated lysis of infected cells (Topham et al., 1997). The efficiency of lysis correlates with the ability to clear an infection (McMichael et al., 1983).

Both convalescent donors and unexposed individuals have SARS-CoV-2-specific T cell responses (Le Bert et al., 2020; Braun et al., 2020; Grifoni et al., 2020b; Mateus et al., 2020; Peng et al., 2020; Tarke et al., 2021; Weiskopf et al., 2020). CD8<sup>+</sup> T cell responses have been identified as correlates of protection in SARS-CoV-2 infection (Chen and John Wherry, 2020; Liao et al., 2020; McMahan et al., 2021). Unexposed individuals may have T cell responses that were generated by common cold human coronaviruses (HCoV) and may be partially protective against SARS-CoV-2 encounter (Lipsitch et al., 2020; Mallajosyula et al., 2021; Mateus et al., 2020). T cells interact with target antigens through the T cell receptor (TCR), which is a heterodimer of alpha and beta chains. TCRs are inherently cross-reactive to maximize the breadth of ligand recognition; however, a single TCR is not guaranteed to recognize related antigens (Sewell, 2012). Several cross-reactive CD8<sup>+</sup> T cell responses are known, but specific TCR $\alpha\beta$  clones that can drive such reactivity are not defined (Lineburg et al., 2021; Lipsitch et al., 2020; Mallajosyula et al., 2021; Mateus et al., 2020). T cell memory is most often defined as ability to recognize synthetic peptide epitopes in functional assays or peptide-major histocompatibility complex (MHC) multimer staining. Recognition of processed epitopes derived from full-length intracellular antigens is underexplored in SARS-CoV-2. Isolation of specific TCR clones permits unambiguous determination of reactivity and detailed characterization of immune responses such as cytotoxic potential and measurement of cross-reactivity against related viruses.

We employ recent technological advances in single-cell sequencing, DNA synthesis, and gene transfer to recover anti-

gen-specific TCR $\alpha\beta$  and subsequently characterize them in allogeneic T cells. The viral polymerase (NSP12/RNA-dependent RNA polymerase [RdRp]) was identified as highly conserved within SARS-CoV-2 and other human coronaviruses. RdRp-reactive CD8<sup>+</sup> T cells were then selected for TCR $\alpha\beta$  droplet-based sequencing (Drop-seq) based on the intracellular level of tumor necrosis factor alpha (TNF $\alpha$ ) and interferon gamma (IFN $\gamma$ ) via mRNA sequencing via cross-linker regulated intracellular phenotype (CLInt-seq), which allows for antigen-specific TCR sequencing via commercially available Drop-seq in cells that are stained for intracellular cytokines (Nesterenko et al., 2021). TCRs were initially screened for single-epitope recognition in a cell line system via the NFAT-GFP reporter system. Reactive TCRs were overexpressed in human peripheral blood mononuclear cells (PBMCs) and killed antigen-presenting cells that expressed the full-length RdRp. Three TCR constructs were broadly reactive and cross-reacted with epitope homologs from HCoV).

## RESULTS

### RdRp is highly conserved among human coronaviruses and within SARS-CoV-2

Antigens derived from highly conserved SARS-CoV-2 proteins should generate immune responses effective against multiple variants. Human coronaviruses are separated by hundreds of years of evolution and serve as a model of the evolutionary constraints that may restrict variant emergence in SARS-CoV-2 (Forni et al., 2017; Killerby et al., 2018). A group of coronavirus proteins involved in RNA synthesis, immune modulation, and structural machinery was selected for further analysis. Sequence identity was compared across all known human coronaviruses. All proteins showed conservation within sub-classes: alpha coronaviruses (229E and NL63), beta coronaviruses (HKU1 and OC43), and both SARS viruses (Figure 1A). The RdRp was most conserved across all coronaviruses (Figure 1A). Across 893,589 SARS-CoV-2 samples sequenced, RdRp was well conserved and had few mutations compared with the spike protein (Figure 1B; Table S4).

### TCRs from unexposed individuals recognize RdRp epitopes

To generate TCR clones, we screened pooled peptide epitopes predicted to bind human leukocyte antigen (HLA)-A\*02:01 against HLA-matched PBMCs collected prior to December of 2019 (Figure 2A). We refer to these samples as unexposed to SARS-CoV-2. CD8<sup>+</sup> T cells that responded by production of TNF $\alpha$  and IFN $\gamma$  were sorted from four different PBMC donors via fluorescence-activated cell sorting (FACS) (Figure 2A). Responses were low in all donors, around the level of background set based on DMSO control stimulation, as would be expected for donors who were not exposed to a specific pathogen.

Reactive cells were sorted for single-cell TCR $\alpha\beta$  sequencing via a highly sensitive technique called CLInt-seq. Clonally expanded TCR clones were synthesized and tested in an allogeneic cell-based system for evaluation of immune receptor activation (Figure 2B). A high-throughput system for TCR reactivity profiling was established (Figure S1A). We utilized a Jurkat cell line that expressed the NFAT-zsGreen T cell activation

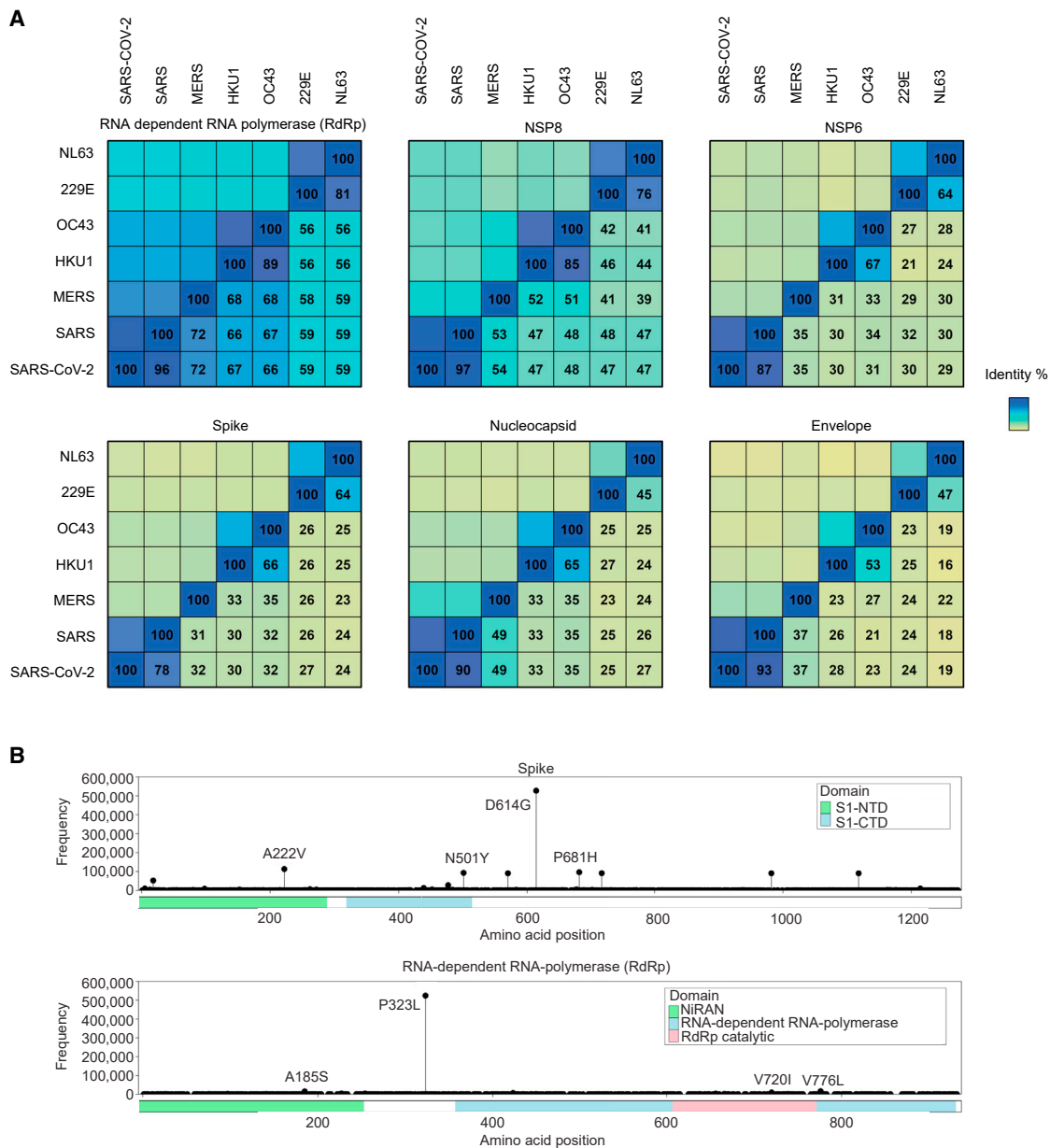


**Figure 1. RdRp is highly conserved among human coronaviruses and within SARS-CoV-2**

(A) Correlation matrix comparing coronavirus protein conservation by amino acid identity across coronaviruses.

(B) Lollipop plots illustrating the distribution and locations of missense variants present in SARS-CoV-2 spike protein and RdRp. Missense variants are highlighted by lollipops and the most frequent variants are labelled in Human Genome Variation Society nomenclature.

reporter construct and the CD8 molecule to stabilize MHC class I interactions. This cell-based reporter system was then optimized with a well-characterized TCR, clone 1G4, which is specific for the cancer antigen NY-ESO-1 (D'Angelo et al., 2018) (Figure S1B). Comparison of TCR delivery by electroporation or viral integration resulted in similar extent of T cell activation (Figure S1C). SARS-CoV-2-specific TCRs were then electroporated or transduced into the Jurkat cell line and activation was measured by FACS measurement of zsGreen. SARS-CoV-2-reactive epitopes were identified via epitope deconvolution

using an array of sub-pools (Figures 2C and S2). Of 44 TCR constructs tested in this system, 10 recognized the cognate peptide pool (Figure 2D). TCR clones that did not score as reactive in this assay either did not reach the threshold of the reporter system or were originally expressed in T cells that did not recognize the queried peptide pool. Because the responses sorted were around the level of background, non-reactive TCRs likely represent the background signal. Nine TCRs clearly recognized four unique epitopes of the RdRp (Figure S2; Table S1).

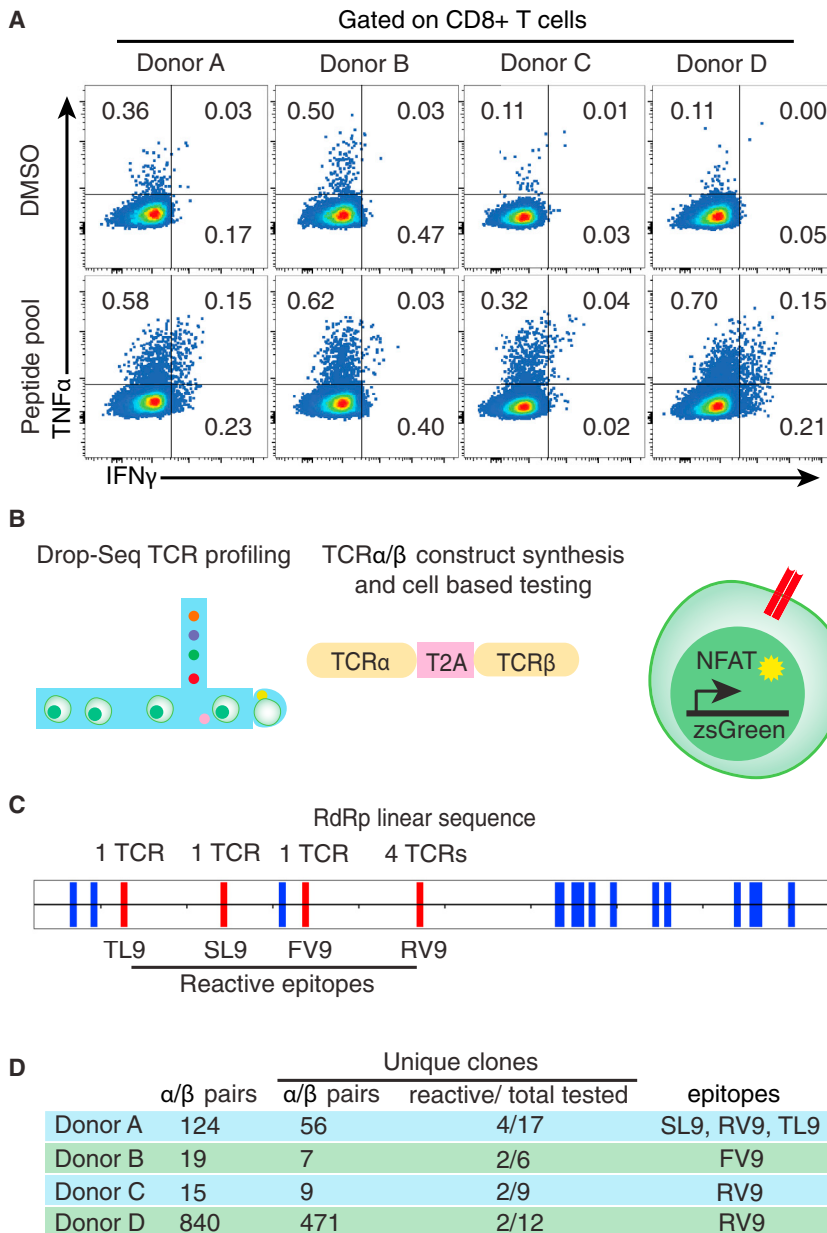


**Figure 2. TCRs from unexposed individuals recognize RdRp epitopes**

(A) FACS sorting analysis of T cells that underwent stimulation by peptide pools and subsequent intracellular staining for TNF $\alpha$  and IFN $\gamma$  using the CLInt-seq protocol, which allows for downstream single-cell TCR $\alpha/\beta$  sequencing. In donors A–C, TNF $\alpha$  and IFN $\gamma$  double-positive cells were selected. For donor D, total fraction of IFN $\gamma$ -positive cells was collected.

(B) Schematic for the TCR $\alpha/\beta$  construct screening in a cell-based reporter system using the NFAT-zsGreen (GFP) reporter.

(C) Epitope map of the RdRp epitopes. Epitopes that reacted with TCR $\alpha/\beta$  constructs are in red, and non-reactive epitopes, which were still part of the pool, are in blue. Number of cognate TCR $\alpha/\beta$  constructs for each of the reactive epitopes is indicated. (D) Summary of reactive TCRs from each of the donors.

of peptide during pulsing assays being supraphysiological (Figure 3D). CD4<sup>+</sup> T cells that overexpressed the coronavirus specific TCR (CoVTCRs) also responded to peptide pulsing but did not recognize processed epitopes. Production of TNF $\alpha$  and IFN $\gamma$  in CD4<sup>+</sup> T cells ranged from 0.058% to 10.3%, depending on the TCR.

T cells control viral spread by killing virus-infected cells. Cytotoxicity assays showed five out of seven TCRs can direct T cells to kill target cell lines (Figure 3E). Recognition of processed epitopes was confirmed by supernatant IFN $\gamma$  ELISA assay (Figure 3F). At 48 h, processed antigen recognition was equivalent to or better than the peptide pulsing control (Figure 3F).

We sought to determine how common RdRp-specific T cells are. Recently, a set of more than 160,000 TCR $\beta$  genes specific for SARS-CoV-2 was made publicly available (Nolan et al., 2020). This data were generated by peptide pool stimulation of

### Isolated TCRs recognize and kill RdRp-expressing cells

Processed antigen recognition is critical for vaccine-induced priming of naive T cell responses as well as for lysis of infected cells. To establish potential antiviral efficacy, seven RdRp-specific TCRs were overexpressed in HLA-A\*02:01-positive human PBMCs via retroviral delivery (Figure 3A; Table S2). Engineered PBMCs were co-cultured with a target cell line engineered to overexpress the full-length SARS-CoV-2 RdRp protein and HLA-A\*02:01 (Figure 3B). The engineered T cells were able to produce TNF $\alpha$  and IFN $\gamma$  in response to recognition of processed antigens (Figures 3C and 3D). Full-length antigen recognition was significantly lower than peptide pulsing, as measured by T cell cytokine production, most likely due to the concentration

PBMCs from 118 donors and subsequent TCR $\beta$  gene sequencing in reactive T cells (Klinger et al., 2015). Unique epitopes were ranked by the count of cognate TCR $\beta$  sequences (Figure S3A). Three of the four epitopes we identified were frequently targeted by the SARS-CoV-2-specific TCR $\beta$  (Figure S3A). GLIPH2, an algorithm for grouping TCRs that recognize the same antigen (Huang et al., 2020), showed three TCR $\alpha/\beta$  constructs we defined grouped with other TCRs against ORF1ab, which contains the RdRp (Figure S3B; Table S3). The epitope FV9 was frequently targeted, but its cognate TCR, CoVTCR 18, did not share sequence similarity with any ORF1ab-specific TCR $\beta$  (Figures S3A and S3B). This TCR also lacked killing ability in the prior assay (Figure 3E). Peptide titration showed that this

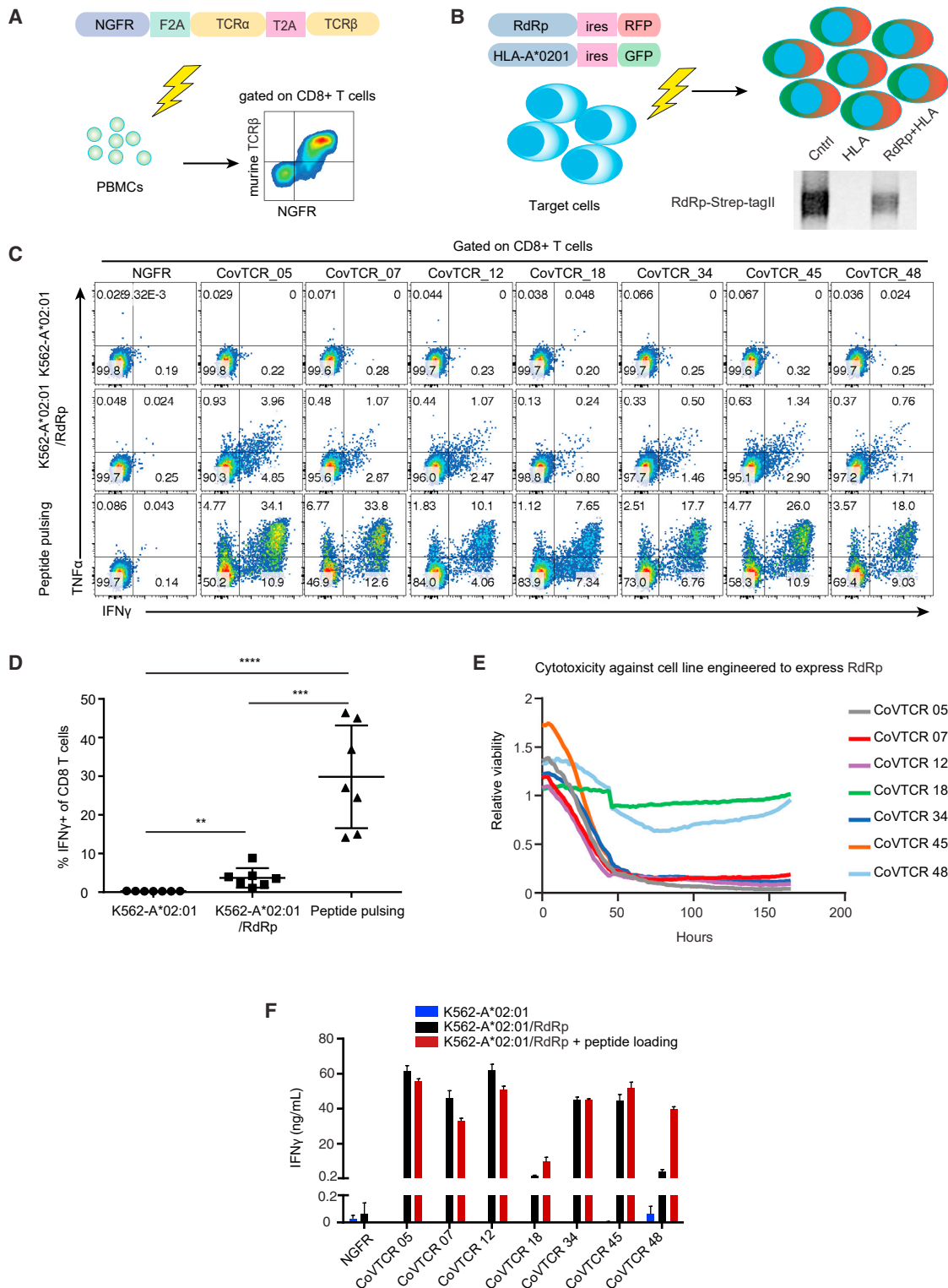


**Figure 3. Isolated TCRs recognize and kill RdRp-expressing cells**

(A) Schematic for generation of human PBMCs that express SARS-CoV-2-reactive TCR $\alpha\beta$  constructs via retrovirus-based construct overexpression. Overexpression is confirmed by Nerve Growth Factor Receptor (NGFR) (secondary marker) and murine TCR $\beta$  constant-region staining by FACS.

(B) Schematic for target cell line generation using the K562 cell line and lentiviral overexpression of the MHC molecule HLA-A\*02:01 and the full-length RdRp sequence that is tagged by Strep-tagII. RdRp expression is confirmed by western blot, where 293T cells transfected with the RdRp vector are the positive control.

(legend continued on next page)

TCR only recognized antigen at high concentration of 10  $\mu\text{g}/\text{mL}$ , confirming that this TCR has low affinity for this specific target (Figure S4). Two of the four TCRs against the RV9 epitope grouped with ORF1ab-specific TCR $\beta$  (Figure S3B). CoVTCR 34, specific against RV9, was strongly cytotoxic but did not group with any TCR $\beta$  by GLIPH2 analysis.

### SARS-CoV-2 RdRp-targeted TCRs broadly recognize human coronaviruses

We then queried RdRp TCR cross-reactivity against the HCoV epitopes. Epitope homologs were identified by alignment of RdRp sequences from all human coronaviruses. Each of the homologous epitopes was synthesized and TCR reactivity against each of the epitopes was profiled via peptide titration assay. RdRp-specific TCR $\alpha\beta$  constructs exhibited a diverse pattern of coronavirus reactivity (Figures 4A–4F). Three TCRs were highly specific for SARS-CoV-2 (Figures 4A, 4B, and 4E). This TCR reactivity may represent the naive T cell repertoire or could be an immune response to unknown antigen. Only two of the four RV9-reactive TCRs recognized one HCoV (Figures 4D and 4F). The TL9-reactive TCR had strong cross-reactivity with SARS, MERS, 229E, and NL63 coronaviruses (Figure 4C).

### DISCUSSION

This study provides a strong basis for considering the development of vaccines against either specific epitopes or the full-length RdRp. Current vaccines provide strong protection against COVID-19 caused by circulating variants of SARS-CoV-2. Continuous evolution of SARS-CoV-2 may necessitate updates to the vaccine's spike sequence, selection of a more conserved antigen, or a combination of both. One of the challenges of developing booster shots is the need to predict which variant will be the most common when the vaccine is administered. Failure to predict this accurately may decrease the efficacy of the booster. SARS-CoV-2 infection can be recognized by RdRp-specific T cells as indicated by strong RdRp CD8<sup>+</sup> T cell responses in convalescent donors (Tarke et al., 2021). The RdRp sequence is particularly well conserved within SARS-CoV-2 and among other human coronaviruses. Sequence conservation suggests that the critical functional role of this protein places restriction on its capacity to evolve. We show that RdRp-specific T cells are cytotoxic against cells that express full-length antigen, which suggests T cell responses against RdRp should help control SARS-CoV-2 infection and prevent COVID-19 disease.

Inducing broadly reactive T cell responses may be particularly important for generating lifelong immunity against SARS-CoV-2. T cells can recognize the target antigen even after accumulation of point mutations (Sewell, 2012). While we identified RdRp as the most conserved protein, it too is likely to change, as evident

from the accumulation of point mutations. Here, we defined two RdRp epitopes that can elicit broadly coronavirus-reactive T cell responses. T cells that recognize different human coronaviruses are likely to recognize novel mutation variants as they emerge, due to strong affinity for the antigen. Epitope TL9-reactive T cells have been previously identified as cross-reactive and associated with reduced disease severity; however, a specific TCR clone driving this response was not identified (Mallajosyula et al., 2021). For the RV9 epitope, some TCRs were cross-reactive but others only recognized SARS-CoV-2, showing that TCRs against the same antigen can have distinct reactivity. The cross-reactive TCRs against RV9 used the same V alpha chain TRAV38-2DV8, implicating that the usage of a common alpha chain may allow cross-reactivity. Specific TCR sequences that are known to allow for broad reactivity can be used as benchmarks for induction of such immunity. TCR-based disease severity correlation will require more TCR characterization to expand the scope of TCRs and HLA allele restrictions. Induction of broadly reactive T cell responses that are not affected by point mutations in the epitope sequence, as well as benchmarks for measurement of such responses, can help guide development of T cell vaccines.

Several reports proposed the use of adoptive transfer of antigen-specific T cells from convalescent donors to treat severe COVID-19 disease (Basar et al., 2021; Ferreras et al., 2020; Keller et al., 2020). Viral infections such as cytomegalovirus (CMV) and Epstein-Barr virus (EBV) have previously been treated by transfer of highly functional cytotoxic T cells (Einsele et al., 2002; Feuchtinger et al., 2010b; Papadopoulou et al., 2014). It remains to be shown whether adoptive transfer of T cells can control SARS-CoV-2 infection in pre-clinical models, which are complicated by the requirement to be done in the Biological Safety Level (BSL) 3 setting. Therapeutic T cell engineering is now routinely done for cancer treatment both in the context of clinical trials as well as US Food and Drug Administration (FDA)-approved therapeutics (D'Angelo et al., 2018; Depil et al., 2020; Johnson et al., 2006). There are several advantages to adoptive cell therapy with engineered T cells: (1) a large number of antigen-specific T cells can be readily produced; (2) well-validated TCR specificity; (3) T cells have a younger phenotype. TCR-engineered T cell also enlist additional CD4<sup>+</sup> T cells, which are critical for establishing long-term CD8<sup>+</sup> T cell memory and antibody production (Sant and McMichael, 2012; Sun and Bevan, 2003). Current approaches for adoptive T cell therapy are expensive and cumbersome (Depil et al., 2020). Technological advances in gene delivery may make T cell engineering a practical approach for viral disease treatment in specific groups of patients (Frank et al., 2020).

A note added in proof: replication complex reactive T cells were recently identified to be protective against seroconversion in health care workers who were likely exposed to SARS-CoV-2

(C) FACS analysis of intracellular staining for TNF $\alpha$  and IFN $\gamma$  in T cells. Cells are gated on light scatter, CD3<sup>+</sup>, CD8<sup>+</sup>.

(D) FACS results from (C) Data from PBMC samples expressing the different TCR constructs are pooled into groups based on the activation stimulus and differences are compared across groups. Student's t test is used to compare the groups: \*\*p > 0.01, \*\*\*p > 0.001, \*\*\*\*p > 0.0001.

(E) PBMC cytotoxicity assay against RdRp-overexpressing target cell line.

(F) IFN $\gamma$  production after 48 h of co-culture of PBMCs and target cell lines expressing RdRp. HLA-A\*02:01-only parental cell line is used as negative control. Error bars represent standard deviation.



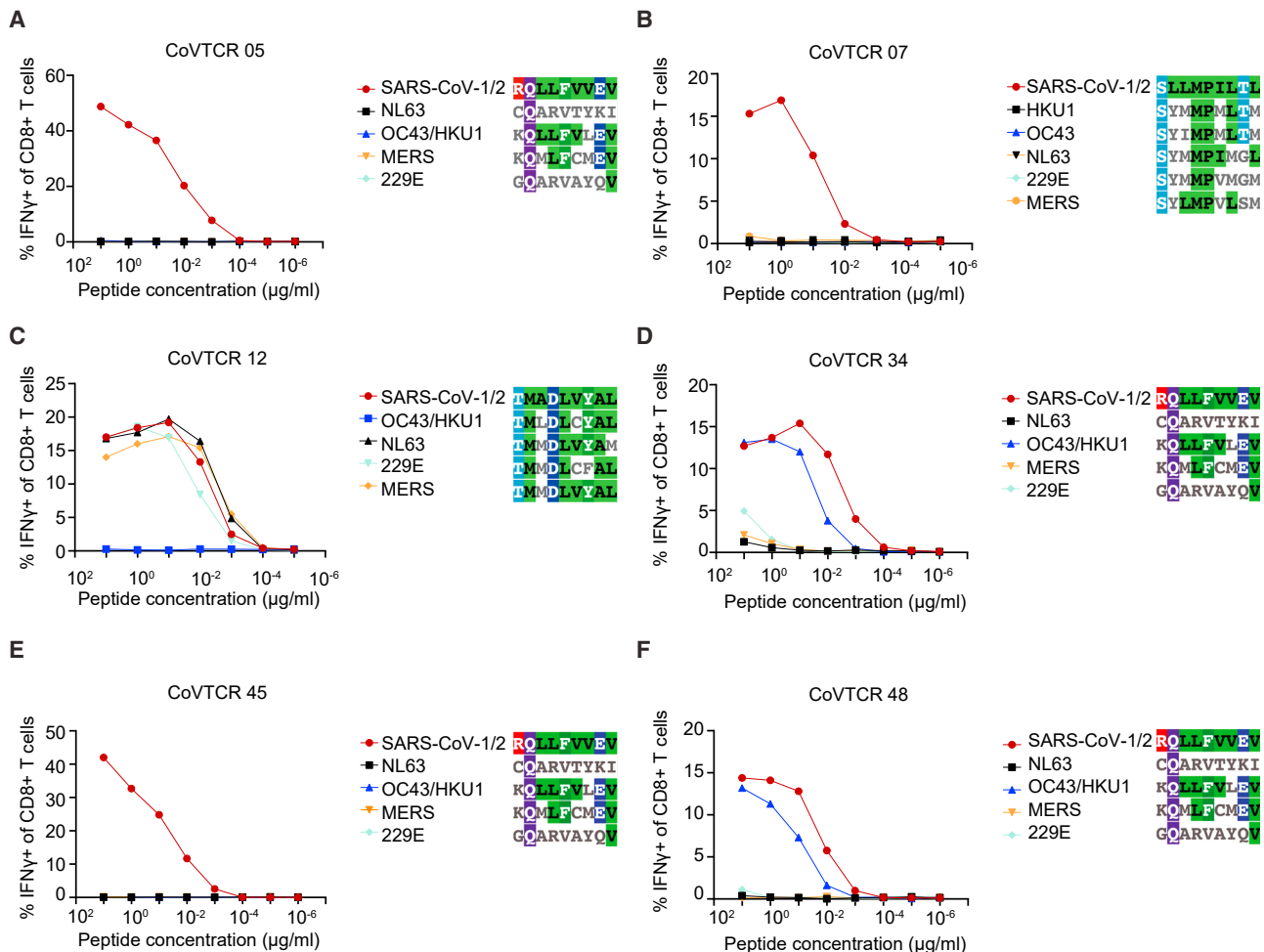


**Figure 4. SARS-CoV-2 RdRp-targeted TCRs broadly recognize human coronaviruses**

Peptide dilution assay to measure reactivity against peptide homologs from HCoVs. PBMCs were engineered to overexpress the TCR $\alpha\beta$  constructs, expanded, and then pulsed with the indicated concentrations of each of the indicated peptide epitopes in the presence of the K562-A\*02:01 to support antigen presentation. Intracellular staining for IFN $\gamma$  is used to measure T cell activation.

(Swadling et al., 2021). The authors suggest that parts of the replication complex, which contains the polymerase, can be used as a vaccine to induce pan-coronavirus cellular immunity. This work is complementary to our findings here.

#### Limitations of the study

We show that RdRp-specific TCRs recognize processed epitopes in a reconstructed system of viral infection; however, we do not show direct control of live SARS-CoV-2. Such an experiment is complicated by the requirement to be done in BSL3 setting. In addition, viruses developed complicated mechanisms to escape T cell effector function, which can make it difficult to detect activity and recognition. T cell function in SARS-CoV-2 is still being investigated, and direct T cell suppression of viral replication has yet to be established. We did not show correlation between T cell responses we identified and disease severity. Such analysis requires a large patient cohort and could indicate the importance of specific T cell responses.

#### STAR★METHODS

Detailed methods are provided in the online version of this paper and include the following:

- KEY RESOURCES TABLE
- RESOURCE AVAILABILITY
  - Lead contact
  - Materials availability
  - Data and code availability
- EXPERIMENTAL MODEL AND SUBJECT DETAILS
  - Cell culture
  - RdRp expressing target cell line generation
- METHOD DETAILS
  - Intracellular staining
  - CLInt-seq
  - Single-cell TCR $\alpha\beta$  sequencing
  - TCR $\alpha\beta$  construct generation and screening
  - Stimulation of Jurkat

- PBMC engineering via retrovirus
- Cytotoxicity analysis
- Antibodies
- Protein conservation analysis
- Lollipop plot generation
- Comparison of TCRs to publicly available data
- **QUANTIFICATION AND STATISTICAL ANALYSIS**

## SUPPLEMENTAL INFORMATION

Supplemental information can be found online at <https://doi.org/10.1016/j.celrep.2021.110167>.

## ACKNOWLEDGMENTS

We thank Michael T. Bethune for providing advice throughout this project, as well as providing the Jurkat-CD8 cells while at the laboratory of David Baltimore (Caltech). The NFAT reporter was a gift from Christopher S. Seet (UCLA) and the laboratory of David Baltimore (Caltech). We thank Caius Radu and Ting-Ting Wu (UCLA) for critical reading of the manuscript. The UCLA Technology Center for Genomics and Bioinformatics constructed single-cell human TCR libraries and performed TCR sequencing. Funding: National Cancer Institute grants U01 CA233074 (O.N.W.) and U24 CA248265 (P.C.B.); Parker Institute for Cancer Immunotherapy grant (O.N.W. and J.R.H.); UCLA Broad Stem Cell Research Center (O.N.W.); USHHS Ruth L. Kirschstein Institutional National Research Service Award T32 CA009056 (P.A.N.); Broad Stem Cell Research Center (BSCRC) predoctoral fellowship (Z.M.); The Jeff and Liesl Wilke Foundation (J.R.H.); The Washington State Andy Hill CARE Fund (J.R.H.); The Biomedical Advanced Research and Development Authority HHSO10201600031C (J.R.H.); UCLA W. M. Keck Foundation COVID-19 Research Award Program (O.N.W.).

## AUTHOR CONTRIBUTIONS

Conceptualization, P.A.N. and O.N.W.; supervision, P.A.N., O.N.W., J.M., J.T.K., J.R.H., P.C.B., and J.W.P.; methodology, M.T.B., P.A.N., P.C.B., J.R.H., W.C., Y.S., L.Y., Z.M., N.J.B., Y.L., D.L., and J.T.K.; investigation, G.B.S., J.M., P.A.N., J.X., R.N., B.L.T., D.C., C.C., and M.N.; funding acquisition, J.W.P., P.C.B., and O.N.W.; software, M.B.O., B.L.T., R.N., and D.Z.; resources, J.X., W.C., and Y.L.; visualization, M.B.O., P.A.N., B.L.T., D.Z., and R.N.; project administration, P.A.N., J.M., and O.N.W.; writing – original draft, review & editing, P.A.N., O.N.W., and J.W.P.

## DECLARATION OF INTERESTS

O.N.W., J.M., and P.A.N. are inventors of a patent application in progress that will be filed prior to manuscript publication. J.R.H. is a board member of PACT Pharma and Isoplexis. O.N.W. currently has consulting, equity, and/or board relationships with Trethera Corporation, Kronos Biosciences, Sofie Biosciences, Breakthrough Properties, Vida Ventures, Nammi Therapeutics, Two River, Iconovir, Appia BioSciences, Neogene Therapeutics, and Allogene Therapeutics. None of these companies contributed to or directed any of the research reported in this article.

Received: August 11, 2021

Revised: October 15, 2021

Accepted: December 2, 2021

Published: December 28, 2021

## REFERENCES

Altschul, S.F., Gish, W., Miller, W., Myers, E.W., and Lipman, D.J. (1990). Basic local alignment search tool. *J. Mol. Biol.* *215*, 403–410.

Anand, S.P., Prévost, J., Nayrac, M., Beaudoin-Bussièrès, G., Benlarbi, M., Gasser, R., Brassard, N., Laumaea, A., Gong, S.Y., Bourassa, C., et al.

(2021). Longitudinal analysis of humoral immunity against SARS-CoV-2 spike in convalescent individuals up to 8 months post-symptom onset. *Cell Rep. Med* *2*, 100290.

Reynisson, B., Alvarez, B., Paul, S., Peters, B., and Nielsen, M. (2020). NetMHCpan-4.1 and NetMHCIIpan-4.0: improved predictions of MHC antigen presentation by concurrent motif deconvolution and integration of MS MHC eluted ligand data. *Nucleic Acids Res.* *48*, W449–W454.

Baden, L.R., El Sahly, H.M., Essink, B., Klotloff, K., Frey, S., Novak, R., Diemert, D., Spector, S.A., Roupael, N., Creech, C.B., et al. (2021). Efficacy and safety of the mRNA-1273 SARS-CoV-2 vaccine. *N. Engl. J. Med.* *384*, 403–416.

Basar, R., Uprety, N., Ensley, E., Daher, M., Klein, K., Martinez, F., Aung, F., Shanley, M., Hu, B., Gokdemir, E., et al. (2021). Generation of glucocorticoid-resistant SARS-CoV-2 T cells for adoptive cell therapy. *Cell Rep* *36*, 109432.

Bernal, J.L., Andrews, N., Gower, C., Gallagher, E., Simmons, R., Thelwall, S., Stowe, J., Tessier, E., Groves, N., Dabrera, G., et al. (2021). Effectiveness of Covid-19 vaccines against the B.1.617.2 (Delta) variant. *N. Engl. J. Med.* *385*, 585–594. <https://doi.org/10.1056/NEJMoa2108891>

Le Bert, N., Tan, A.T., Kunasegaran, K., Tham, C.Y.L., Hafezi, M., Chia, A., Chng, M.H.Y., Lin, M., Tan, N., Linster, M., et al. (2020). SARS-CoV-2-specific T cell immunity in cases of COVID-19 and SARS, and uninfected controls. *Nature* *584*, 457.

Bethune, M.T., Li, X.-H., Yu, J., McLaughlin, J., Cheng, D., Mathis, C., Moreno, B.H., Woods, K., Knights, A.J., and Garcia-Diaz, A. (2018). Isolation and characterization of NY-ESO-1-specific T cell receptors restricted on various MHC molecules. *Proc. Natl. Acad. Sci.* *115*, E10702–E10711.

Braun, J., Loyal, L., Frensch, M., Wendisch, D., Georg, P., Kurth, F., Hippenstiel, S., Dingeldey, M., Kruse, B., Fauchere, F., et al. (2020). SARS-CoV-2-reactive T cells in healthy donors and patients with COVID-19. *Nature* *587*, 270–274.

Chen, Z., and John Wherry, E. (2020). T cell responses in patients with COVID-19. *Nat. Rev. Immunol.* *20*, 529–536.

D’Angelo, S.P., Melchiori, L., Merchant, M.S., Bernstein, D., Glod, J., Kaplan, R., Grupp, S., Tap, W.D., Chagin, K., Binder, G.K., et al. (2018). Antitumor activity associated with prolonged persistence of adoptively transferred NY-ESO-1 c259T cells in synovial sarcoma. *Cancer Discov.* *8*, 944–957.

Depil, S., Duchateau, P., Grupp, S.A., Mufti, G., and Poirot, L. (2020). ‘Off-the-shelf’ allogeneic CAR T cells: development and challenges. *Nat. Rev. Drug Discov.* *19*, 185–199.

Dutta, N.K., Mazumdar, K., and Gordy, J.T. (2020). The nucleocapsid protein of SARS-CoV-2: a target for vaccine development. *J. Virol.* *94*, e00620–e00647.

Einsele, H., Roosnek, E., Rufer, N., Sinzger, C., Riegler, S., Löffler, J., Grigoleit, U., Moris, A., Rammensee, H.-G., Kanz, L., et al. (2002). Infusion of cytomegalovirus (CMV)-specific T cells for the treatment of CMV infection not responding to antiviral chemotherapy. *Blood* *99*, 3916–3922.

Ferreras, C., Pascual-Miguel, B., Mestre-Durán, C., Navarro-Zapata, A., Clares-Villa, L., Martín-Cortázar, C., de Paz, R., Marcos, A., Vicario, J.L., Balas, A., et al. (2020). SARS-CoV-2 specific memory T lymphocytes from COVID-19 convalescent donors: identification, biobanking and large-scale production for adoptive cell therapy. *BioRxiv* *2020*, 352294. <https://doi.org/10.3389/fcell.2021.620730>.

Feuchtinger, T., Opherk, K., Bethge, W.A., Topp, M.S., Schuster, F.R., Weisinger, E.M., Mohty, M., Or, R., Maschan, M., Schumm, M., et al. (2010a). Adoptive transfer of pp65-specific T cells for the treatment of chemorefractory cytomegalovirus disease or reactivation after haploidentical and matched unrelated stem cell transplantation. *Blood* *116*, 4267–4360.

Feuchtinger, T., Opherk, K., Bethge, W.A., Topp, M.S., Schuster, F.R., Weisinger, E.M., Mohty, M., Or, R., Maschan, M., Schumm, M., et al. (2010b). Adoptive transfer of pp65-specific T cells for the treatment of chemorefractory cytomegalovirus disease or reactivation after haploidentical and matched unrelated stem cell transplantation. *Blood* *116*, 4360–4367.

Forni, D., Cagliani, R., Clerici, M., and Sironi, M. (2017). Molecular evolution of human coronavirus genomes. *Trends Microbiol.* *25*, 35–48.

- Frank, A.M., Braun, A.H., Scheib, L., Agarwal, S., Schneider, I.C., Fusil, F., Perian, S., Sahin, U., Thalheimer, F.B., Verhoeven, E., et al. (2020). Combining T-cell-specific activation and *in vivo* gene delivery through CD3-targeted lentiviral vectors. *Blood Adv.* **4**, 5702–5715.
- Gauttier, V., Morello, A., Girault, I., Mary, C., Belarif, L., Desselle, A., Wilhelm, E., Bourquard, T., Pengam, S., Teppaz, G., et al. (2020). Tissue-resident memory CD8 T-cell responses elicited by a single injection of a multi-target COVID-19 vaccine. *BioRxiv*. <https://doi.org/10.1101/2020.08.14.240093>.
- Gordon, D.E., Jang, G.M., Bouhaddou, M., Xu, J., Obernier, K., White, K.M., O'Meara, M.J., Rezelj, V.V., Guo, J.Z., Swaney, D.L., et al. (2020). A SARS-CoV-2 protein interaction map reveals targets for drug repurposing. *Nature* **583**, 459–468.
- Grifoni, A., Sidney, J., Zhang, Y., Scheuermann, R.H., Peters, B., and Sette, A. (2020a). A sequence homology and bioinformatic approach can predict candidate targets for immune responses to SARS-CoV-2. *Cell Host Microbe* **27**, 671–680.e2.
- Grifoni, A., Weiskopf, D., Ramirez, S.I., Mateus, J., Dan, J.M., Moderbacher, C.R., Rawlings, S.A., Sutherland, A., Premkumar, L., Jadi, R.S., et al. (2020b). Targets of T cell responses to SARS-CoV-2 coronavirus in humans with COVID-19 disease and unexposed individuals. *Cell* **181**, 1489–1501.e15.
- Hall, C.B., Powell, K.R., MacDonald, N.E., Gala, C.L., Menegus, M.E., Suffin, S.C., and Cohen, H.J. (1986). Respiratory syncytial viral infection in children with compromised immune function. *N. Engl. J. Med.* **315**, 77–81.
- Harty, J.T., Tvinnereim, A.R., and White, D.W. (2000). Cd8+ T cell effector mechanisms in resistance to infection. *Annu. Rev. Immunol.* **18**, 275–308.
- Harvey, W.T., Carabelli, A.M., Jackson, B., Gupta, R.K., Thomson, E.C., Harrison, E.M., Ludden, C., Reeve, R., Rambaut, A., Peacock, S.J., et al. (2021). SARS-CoV-2 variants, spike mutations and immune escape. *Nat. Rev. Microbiol.* **19**, 409–424.
- Hatcher, E.L., Zhdanov, S.A., Bao, Y., Blinkova, O., Nawrocki, E.P., Ostapchuk, Y., Schaffer, A.A., and Rodney Brister, J. (2017). Virus variation resource-improved response to emergent viral outbreaks. *Nucleic Acids Res.* **45**, D482–D490.
- Hoffmann, M., Arora, P., Groß, R., Seidel, A., Hörnich, B.F., Hahn, A.S., Krüger, N., Graichen, L., Hofmann-Winkler, H., Kempf, A., et al. (2021). SARS-CoV-2 variants B.1.351 and P.1 escape from neutralizing antibodies. *Cell* **184**, 2384–2393.e12.
- Huang, H., Wang, C., Rubelt, F., Scriba, T.J., and Davis, M.M. (2020). Analyzing the *Mycobacterium tuberculosis* immune response by T-cell receptor clustering with GLIPH2 and genome-wide antigen screening. *Nat. Biotechnol.* **38**, 1194–1202.
- Johnson, L.A., Heemskerck, B., Powell, D.J., Cohen, C.J., Morgan, R.A., Dudley, M.E., Robbins, P.F., and Rosenberg, S.A. (2006). Gene transfer of tumor-reactive TCR confers both high avidity and tumor reactivity to nonreactive peripheral blood mononuclear cells and tumor-infiltrating lymphocytes. *J. Immunol.* **177**, 6548–6559.
- Jozwik, A., Habibi, M.S., Paras, A., Zhu, J., Guvenel, A., Dhariwal, J., Almond, M., Wong, E.H.C., Sykes, A., Maybeno, M., et al. (2015). RSV-specific airway resident memory CD8+ T cells and differential disease severity after experimental human infection. *Nat. Commun.* **6**, 10224.
- Keller, M.D., Harris, K.M., Jensen-Wachspress, M.A., Kankate, V.V., Lang, H., Lazarski, C.A., Durkee-Shock, J., Lee, P.H., Chaudhry, K., Webber, K., et al. (2020). SARS-CoV-2-specific T cells are rapidly expanded for therapeutic use and target conserved regions of the membrane protein. *Blood* **136**, 2905–2917.
- Khoury, D.S., Cromer, D., Reynaldi, A., Schlub, T.E., Wheatley, A.K., Juno, J.A., Subbarao, K., Kent, S.J., Triccas, J.A., and Davenport, M.P. (2021). Neutralizing antibody levels are highly predictive of immune protection from symptomatic SARS-CoV-2 infection. *Nat. Med.* **27**, 1205–1211.
- Killerby, M.E., Biggs, H.M., Haynes, A., Dahl, R.M., Mustaqim, D., Gerber, S.I., and Watson, J.T. (2018). Human coronavirus circulation in the United States 2014–2017. *J. Clin. Virol.* **101**, 52–56.
- Klinger, M., Pepin, F., Wilkins, J., Asbury, T., Wittkop, T., Zheng, J., Moorhead, M., and Faham, M. (2015). Multiplex identification of antigen-specific T cell receptors using a combination of immune assays and immune receptor sequencing. *PLoS One* **10**, e0141561.
- Kuzmina, A., Khalaila, Y., Voloshin, O., Keren-Naus, A., Boehem, L., Raviv, Y., Shemer-Avni, Y., Rosenberg, E., and Taube, R. (2021). SARS CoV-2 spike variants exhibit differential infectivity and neutralization resistance to convalescent or post-vaccination sera. *Cell Host Microbe* **29**, 522–528.e2.
- Liao, M., Liu, Y., Yuan, J., Wen, Y., Xu, G., Zhao, J., Cheng, L., Li, J., Wang, X., Wang, F., et al. (2020). Single-cell landscape of bronchoalveolar immune cells in patients with COVID-19. *Nat. Med.* **26**, 842–844.
- Lineburg, K.E., Grant, E.J., Swaminathan, S., Chatzileontiadou, D.S., Szeto, C., Sloane, H., Panikkar, A., Raju, J., Crooks, P., Rehan, S., et al. (2021). CD8+ T cells specific for an immunodominant SARS-CoV-2 nucleocapsid epitope cross-react with selective seasonal coronaviruses. *Immunity* **54**, 1055–1065.e5.
- Lipsitch, M., Grad, Y.H., Sette, A., and Crotty, S. (2020). Cross-reactive memory T cells and herd immunity to SARS-CoV-2. *Nat. Rev. Immunol.* **20**, 709–713.
- Lumley, S.F., O'Donnell, D., Stoesser, N.E., Matthews, P.C., Howarth, A., Hatch, S.B., Marsden, B.D., Cox, S., James, T., Warren, F., et al. (2020). Antibody status and incidence of SARS-CoV-2 infection in health care workers. *N. Engl. J. Med.* **384**, 533–540. <https://doi.org/10.1056/NEJMoa2034545>.
- Madeira, F., Park, Y.M., Lee, J., Buso, N., Gur, T., Madhusoodanan, N., Basutkar, P., Tivey, A.R.N., Potter, S.C., Finn, R.D., et al. (2019). The EMBL-EBI search and sequence analysis tools APIs in 2019. *Nucleic Acids Res.* **47**, W636–W641.
- Mallajosyula, V., Ganjavi, C., Chakraborty, S., McSweeney, A.M., Pavlovitch-Bedzyk, A.J., Wilhelmy, J., Nau, A., Manohar, M., Nadeau, K.C., and Davis, M.M. (2021). CD8+ T cells specific for conserved coronavirus epitopes correlate with milder disease in COVID-19 patients. *Sci. Immunol.* **6**, eabg5669.
- Mateus, J., Grifoni, A., Tarke, A., Sidney, J., Ramirez, S.I., Dan, J.M., Burger, Z.C., Rawlings, S.A., Smith, D.M., Phillips, E., et al. (2020). Selective and cross-reactive SARS-CoV-2 T cell epitopes in unexposed humans. *Science* **370**, 89–94.
- McMahan, K., Yu, J., Mercado, N.B., Loos, C., Tostanoski, L.H., Chandrashekar, A., Liu, J., Peter, L., Atyeo, C., Zhu, A., et al. (2021). Correlates of protection against SARS-CoV-2 in rhesus macaques. *Nature* **590**, 630–634.
- McMichael, A.J., Gotch, F.M., Noble, G.R., and Beare, P.A.S. (1983). Cytotoxic T-cell immunity to influenza. *N. Engl. J. Med.* **309**, 13–17.
- Muik, A., Wallisch, A.K., Sängler, B., Swanson, K.A., Mühl, J., Chen, W., Cai, H., Maurus, D., Sarkar, R., Türeci, Ö., et al. (2021). Neutralization of SARS-CoV-2 lineage B.1.1.7 pseudovirus by BNT162b2 vaccine-elicited human sera. *Science* **371**, 1152–1153.
- Nesterenko, P.A., McLaughlin, J., Cheng, D., Bangayan, N.J., Sojo, G.B., Seet, C.S., Qin, Y., Mao, Z., Obusan, M.B., Phillips, J.W., et al. (2021). Droplet-based mRNA sequencing of fixed and permeabilized cells by CLInt-seq allows for antigen-specific TCR cloning. *Proc. Natl. Acad. Sci. U. S. A.* **118**, e2021190118.
- Nolan, S., Vignali, M., Klinger, M., Dines, J.N., Kaplan, I.M., Svejnova, E., Craft, T., Boland, K., Pesesky, M., Gittelman, R.M., et al. (2020). A large-scale database of T-cell receptor beta (TCRβ) sequences and binding associations from natural and synthetic exposure to SARS-CoV-2. *Res. Sq.*, rs-51964.
- P'ng, C., Green, J., Chong, L.C., Waggott, D., Prokopec, S.D., Shamsi, M., Nguyen, F., Mak, D.Y.F., Lam, F., Albuquerque, M.A., et al. (2019). BPG: seamless, automated and interactive visualization of scientific data. *BMC Bioinformatics* **20**, 1–5.
- Papadopoulou, A., Gerdemann, U., Katari, U.L., Tzannou, I., Liu, H., Martinez, C., Leung, K., Carrum, G., Gee, A.P., Vera, J.F., et al. (2014). Activity of broad-spectrum T cells as treatment for AdV, EBV, CMV, BKV, and HHV6 infections after HSCT. *Sci. Transl. Med.* **6**, 242ra83.
- Peng, Y., Mentzer, A.J., Liu, G., Yao, X., Yin, Z., Dong, D., Dejnirattaisai, W., Rostron, T., Supasa, P., Liu, C., et al. (2020). Broad and strong memory

- CD4<sup>+</sup> and CD8<sup>+</sup> T cells induced by SARS-CoV-2 in UK convalescent individuals following COVID-19. *Nat. Immunol.* **21**, 1336–1345.
- Planas, D., Veyer, D., Baidaliuk, A., Staropoli, I., Guivel-Benhassine, F., Rajah, M.M., Planchais, C., Porrot, F., Robillard, N., Puech, J., et al. (2021). Reduced sensitivity of SARS-CoV-2 variant Delta to antibody neutralization. *Nat.* **2021**, 1–7.
- Polack, F.P., Thomas, S.J., Kitchin, N., Absalon, J., Gurtman, A., Lockhart, S., Perez, J.L., Pérez Marc, G., Moreira, E.D., Zerbini, C., et al. (2020). Safety and efficacy of the BNT162b2 mRNA covid-19 vaccine. *N. Engl. J. Med.* **383**, 2603–2615.
- Poran, A., Harjanto, D., Malloy, M., Arieta, C.M., Rothenberg, D.A., Lenkala, D., van Buuren, M.M., Addona, T.A., Rooney, M.S., Srinivasan, L., et al. (2020). Sequence-based prediction of SARS-CoV-2 vaccine targets using a mass spectrometry-based bioinformatics predictor identifies immunogenic T cell epitopes. *Genome Med.* **12**, 1–15.
- Sadoff, J., Gray, G., Vandebosch, A., Cárdenas, V., Shukarev, G., Grinsztejn, B., Goepfert, P.A., Truyers, C., Fennema, H., Spiessens, B., et al. (2021). Safety and efficacy of single-dose Ad26.COV2.S vaccine against Covid-19. *N. Engl. J. Med.* **384**, 2187–2201. <https://doi.org/10.1056/NEJMoa2101544>.
- Sant, A.J., and McMichael, A. (2012). Revealing the role of CD4<sup>+</sup> T cells in viral immunity. *J. Exp. Med.* **209**, 1391–1395.
- Seet, C.S., He, C., Bethune, M.T., Li, S., Chick, B., Gschweng, E.H., Zhu, Y., Kim, K., Kohn, D.B., Baltimore, D., et al. (2017). Generation of mature T cells from human hematopoietic stem and progenitor cells in artificial thymic organoids. *Nat. Methods* **14**, 521–530.
- Sewell, A.K. (2012). Why must T cells be cross-reactive? *Nat. Rev. Immunol.* **12**, 669–677.
- Shu, Y., and McCauley, J. (2017). GISAIID: global initiative on sharing all influenza data – from vision to reality. *Eurosurveillance* **22**, 30494.
- Sieling, P., King, T., Wong, R., Nguyen, A., Wnuk, K., Rice, A., Adisetiyo, H., Hermreck, M., Verma, M., Zakin, L., et al. (2021). Single prime hAd5 spike (S) + nucleocapsid (N) dual antigen vaccination of 1 healthy volunteers induces a ten-fold increase in mean S- and N-T-cell responses 2 equivalent to T-cell responses from patients previously infected with SARS-CoV-2 3 4. *MedRxiv*. <https://doi.org/10.1101/2021.04.05.21254940>.
- Singer, J.B., Gifford, R.J., Cotten, M., and Robertson, D.L. (2020). CoV-GLUE: a Web Application for Tracking SARS-CoV-2 Genomic Variation. <https://doi.org/10.20944/preprints202006.0225.v1>.
- Sun, J.C., and Bevan, M.J. (2003). Defective CD8 T cell memory following acute infection without CD4 T cell help. *Science* **300**, 339–342.
- Swadling, L., Diniz, M.O., Schmidt, N.M., Amin, O.E., Chandran, A., Shaw, E., Pade, C., Gibbons, J.M., Le Bert, N., Tan, A.T. and Jeffery-Smith, A., 2021. Pre-existing polymerase-specific T cells expand in abortive seronegative SARS-CoV-2. *Nature*, pp.1-10.Vancouver
- Tarke, A., Sidney, J., Kidd, C.K., Dan, J.M., Ramirez, S.I., Yu, E.D., Mateus, J., da Silva Antunes, R., Moore, E., Rubiro, P., et al. (2021). Comprehensive analysis of T cell immunodominance and immunoprevalence of SARS-CoV-2 epitopes in COVID-19 cases. *Cell Rep. Med* **2**.
- Topham, D.J., Tripp, R.A., and Doherty, P.C. (1997). CD8<sup>+</sup> T cells clear influenza virus by perforin or Fas-dependent processes. *J. Immunol.* **159**, 100204.
- Wang, P., Nair, M.S., Liu, L., Iketani, S., Luo, Y., Guo, Y., Wang, M., Yu, J., Zhang, B., Kwong, P.D., et al. (2021). Antibody resistance of SARS-CoV-2 variants B.1.351 and B.1.1.7. *BioRxiv*. <https://doi.org/10.1101/2021.01.25.428137>.
- Weiskopf, D., Schmitz, K.S., Raadsen, M.P., Grifoni, A., Okba, N.M.A., Endeman, H., van den Akker, J.P.C., Molenkamp, R., Koopmans, M.P.G., van Gorp, E.C.M., et al. (2020). Phenotype and kinetics of SARS-CoV-2-specific T cells in COVID-19 patients with acute respiratory distress syndrome. *Sci. Immunol.* **5**, 2071.

STAR★METHODS

KEY RESOURCES TABLE

REAGENT or RESOURCE	SOURCE	IDENTIFIER
<b>Antibodies</b>		
NGFR-PECy7	Biologend	CAT# 345110, RRID:AB_11203542
murine TCRβ-APC	Biologend	CAT# 109212, RRID:AB_313435
CD3-APCCy7	Thermo Fisher	CAT# 47-0036-42, RRID:AB_10717514
CD8a-PE	Thermo Fisher	CAT# 12-0088-42, RRID:AB_1724104
CD4-PECy7	Biologend	CAT# 300512, RRID:AB_314080
IFNγ-APC	Biologend	CAT# 506510, RRID:AB_315443
TNFα-FITC	Biologend	CAT# 502906, RRID:AB_315258
HLA-A2-APC	Thermo Fisher	CAT# 17-9876-42, RRID:AB_11149299
anti-Strep-tag II	Abcam	CAT# ab180957
goat anti-rabbit IgG HRP	Bio-Rad	CAT#170-6515
<b>Bacterial and virus strains</b>		
NFAT-zsGreen virus	UCLA, Christopher Seet "this paper"	N/A
<b>Biological samples</b>		
Human PBMCs	Allcells	N/A
Human PBMCs	Hemacare	N/A
Human PBMCs	UCLA core	N/A
<b>Chemicals, peptides, and recombinant proteins</b>		
Custom synthetic peptides	Elim Biopharma	N/A
IL-2	Peprtech	CAT# 200-02
10X PBS	Fisher Scientific	CAT# MT-46013CM
FBS	Omega Scientific	CAT# FB-11
AIM V media	Thermo Fisher	CAT# 12055083
Human AB serum	Omega Scientific	CAT# HS-20
IL-15	Peprtech	CAT# 200-15
CD28/CD49d	BD Biosciences	CAT# 347690, RRID:AB_647457
Brefeldin A	Biologend	CAT# 420601
pMAX vector	Lonza	CAT# VDC-1040
RPMI 1640	Thermo Fisher	CAT# 31800089
Sodium Pyruvate	Thermo Fisher	CAT# 11360070
HEPES	Thermo Fisher	CAT# 15630130
non-essential amino acids	Thermo Fisher	CAT# 11140050
β-mercaptoethanol	Sigma	CAT# M3148
Polybrene	Sigma-Aldrich	CAT# H9268
DSP	Thermo Fisher	CAT# 22586
RNAsin plus	Promega	CAT# N2615
1M Tris	Thermo Fisher	CAT# AM9850G
Molecular grade DMSO	Sigma	CAT# D8418-50ML
Penicillin-Streptomycin	Omega Scientific	CAT# PS-20
Nuclease free water	Thermo Fisher	CAT# AM9939
Nuclease free BSA	Gemini	CAT# 700-106P
Triton X-100	Sigma	CAT# T8787
Glutamax	Thermo Fisher	CAT# 35050061

(Continued on next page)

**Continued**

REAGENT or RESOURCE	SOURCE	IDENTIFIER
<b>Critical commercial assays</b>		
Lonza 4D Nucleofactor	Lonza	CAT# AAF-1002B
SE cell Line kit S	Lonza	CAT# V4XC-1032
QIAprep miniprep kit	Qiagen	CAT# 27106
CD3/CD28 beads	Thermo Fisher	CAT# 11132D
Cytofix/Cytoperm kit	BD Biosciences	CAT# 554714
single-cell VDJ V1.0 and V1.1	10X Genomics	N/A
OptEIA Reagent Set B	BD Biosciences	CAT# 550534, RRID: AB_2868891
OptEIA human IFN- $\gamma$	BD Biosciences	CAT# 555142, RRID: AB_2869029
IncuCyte system	Sartorius	N/A
<b>Experimental models: Cell lines</b>		
K562	ATCC	CAT# CCL-243, RRID: CVCL_0004
293T	ATCC	CAT# CRL-3216, RRID: CVCL_0063
Jurkat-CD8	Caltech, David Baltimore (Bethune et al., 2018)	N/A
K562-A2/RdRp	This paper	N/A
Jukrat-CD8/NFAT-zsGreen	This paper	N/A
<b>Oligonucleotides</b>		
Custom synthetic DNA	Twist, Table S2	N/A
Custom synthetic DNA	IDT, Table S2	N/A
<b>Recombinant DNA</b>		
NSP12 plasmid	Addgene	plasmid # 141378, RRID:Addgene_141378
RdRp reactive TCR sequences	This paper	N/A
<b>Software and algorithms</b>		
FlowJo	Tree Star Inc.	N/A
GraphPad Prism	GraphPad Software	N/A
R	R	N/A
GLIPH2	(Huang et al., 2020)	N/A

**RESOURCE AVAILABILITY**

**Lead contact**

Further information and requests for resources and reagents should be directed to and will be fulfilled by the lead contact, Owen N. Witte ([owenwitte@mednet.ucla.edu](mailto:owenwitte@mednet.ucla.edu)).

**Materials availability**

We generated unique TCR sequences. The full-length TCR clone sequences are provided in this paper. Any cell line that we created and used is available to other investigators.

**Data and code availability**

Reactive TCR alpha/beta nucleotide sequences are provided in this paper.

We have not created any original code.

Any additional information required to reanalyze the data reported in this paper is available from the lead contact upon request.

**EXPERIMENTAL MODEL AND SUBJECT DETAILS**

**Cell culture**

Cryo preserved peripheral blood mononuclear cells (PBMCs) were commercially purchased (Allcells and Hemacare) or obtained from the CFAR Virology Core Laboratory at the UCLA AIDS Institute. PBMCs were thawed in a water bath set to 37C, transferred to 50 mL

conical tube, 1 mL of warm R10 media was added drop wise and then 14 mL R10 were added. Cells were then centrifuged at 1300 RPM for 7 minutes. To isolate reactive T cells, peripheral blood mononuclear cells (PBMCs) (Allcells and Hemacare) were cultured in TCRPMI media: RPMI 1640 (Thermo Fisher), 10% FBS (Omega Scientific), 1X Glutamax (Thermo Fisher), 1X Sodium Pyruvate (Thermo Fisher), 10 mM HEPES (Thermo Fisher), 1X non-essential amino acids (Thermo Fisher), 50  $\mu$ M  $\beta$ -mercaptoethanol (Sigma) and Penicillin-Streptomycin (Omega Scientific). PBMCs were cultured for 8 days in the presence of peptide pools at 1  $\mu$ g/ml and 25 U/mL of IL-2 (Peprotech) as previously described (Nesterenko et al., 2021). PBMCs were then washed two times in PBS (Fisher Scientific), once in TCRPMI and then plated for 12-h rest in 96-well U bottom plates. Jurkat cells were cultured in R10: 1640 RPMI (Thermo Fisher) supplemented with 10% FBS (Omega Scientific) and 1X Glutamax (Thermo Fisher). An NFAT-zsGreen reporter construct was overexpressed in the Jurkat CD8 cell line. Both NFAT-zsGreen plasmid and the Jurkat CD8 cell line were gifts from the David Baltimore lab. K562 (ATCC) cells were cultured in R10. PBMC for TCR engineering experiments were cultured in AIM V media (Thermo Fisher) supplemented with 5% Human AB serum (Omega Scientific), 50 U/mL of IL-2, 1ng/mL IL-15 (Peprotech), 1X Glutamax and 50 $\mu$ M  $\beta$ -mercaptoethanol. For functional experiments with engineered PBMCs supplemented AIM V media without IL-2 and IL-15 was used. 293T (ATCC) cells were cultured in DMEM (Thermo Fisher) supplemented with 1X Glutamax or Glutamine (Fisher Scientific) and 10% FBS.

### RdRp expressing target cell line generation

pLVX-EF1alpha-SARS-CoV-2-nsp12-2xStrep-IRES-Puro was a gift from Nevan Krogan (Addgene plasmid # 141,378; <http://n2t.net/addgene:141378>; RRID:Addgene\_141,378) (Gordon et al., 2020). RNA-dependent RNA-polymerase (RdRp/NSP12) sequence was subcloned into a third-generation lentivirus packaging vector MNDU-3-ires-Strawberry. Lentivirus was produced as described previously (Seet et al., 2017). Lentivirus was used to infect K562-HLA-A\*02:01 cells that were described by us previously (Bethune et al., 2018). To ensure stable expression of RdRp and HLA-A\*02:01 in K562 cells, single cells were cloned by FACS deposition and selected for high levels of RFP and GFP. Stable RdRp protein level was confirmed by Western blot using anti-Strep-tag II antibody (Abcam, 1:500) and goat anti-rabbit-IgG HRP (Bio-Rad, 1:5000). These single cell clones were used for the cytotoxicity assay.

## METHOD DETAILS

### Intracellular staining

RdRp HLA-A\*02:01 restricted epitopes were identified by prior publications and or prediction by the netMHCpan4.0 (B et al., 2020; Grifoni et al., 2020a; Poran et al., 2020; Reynisson et al., 2020). PBMCs were stimulated in 96 well U bottom plates with 10  $\mu$ g/mL of peptide and 1  $\mu$ g/mL of CD28/CD49d antibodies (BD Biosciences). For peptide titration assays, serial dilution was set up where the original 10  $\mu$ g/mL concentration was diluted 10 fold for every subsequent dilution. For recognition of processed antigen, PBMCs were stimulated with target cell lines without peptide at a 4:1 effector to target ratio. After 1 h, 1X Brefeldin A (Biolegend) was added. Cells were then incubated for 8 more hours after which they were either processed or moved to 4C. For analytical assays, cells were stained for surface markers CD3, CD4, CD8 and intracellular markers TNF $\alpha$  and IFN $\gamma$  using the Cytotfix/Cytoperm kit (BD Biosciences).

### CLInt-seq

For TCR $\alpha\beta$  sequencing via the CLInt-Seq staining we followed our previously published protocol (Nesterenko et al., 2021). Cells were stimulated as described above for intracellular staining. PBS was made from 10X PBS and nuclease free water (Thermo Fisher). All buffers, except for DSP, contained RNAsin (Promega) at 1:400 dilution. Cells were washed twice with staining buffer: nuclease free PBS (Fisher scientific), 1% nuclease free BSA (Gemini) and 1:400 RNAsin plus (Promega). Cells were then stained for 15 min in buffer for surface antigens and subsequently washed once with staining buffer and twice with PBS. DSP was then added to each well at 0.25 mg/mL in 200  $\mu$ L of PBS for 30 min at room temperature. The reaction was quenched with 20  $\mu$ L of 200mM TRIS (Thermo Fisher). Cells were then washed twice with buffer and incubated with 100  $\mu$ L of 0.05% Triton X-100 (Sigma) for 10 min on ice. Cells were then washed and incubated with antibodies against TNF $\alpha$  and IFN $\gamma$  for 20 min on ice in 100  $\mu$ L of buffer, followed by a final wash step. Cells were gated on light scatter, CD3+, CD8+/CD4- to analyze TNF $\alpha$  and IFN $\gamma$  signal. For TCR sequencing cells were either sorted on TNF $\alpha$ /IFN $\gamma$  double-positive cells or IFN $\gamma$  positive cells.

### Single-cell TCR $\alpha\beta$ sequencing

TNF $\alpha$  and IFN $\gamma$ -producing CD8+ T cells were sorted by FACS into a 2 mL Eppendorf tube as described previously (Nesterenko et al., 2021). Sorted cells were then resuspended in 30 to 60  $\mu$ L in .04% BSA solution with RNAsin, to reach a concentration of more than 100 cells/ $\mu$ L. To achieve such concentration, similarly processed Jurkat cells were added as a carrier cell population. Human TCR VDJ libraries were then constructed by the UCLA Technology Center for Genomics & Bioinformatics using the single-cell VDJ V1.0 and V1.1 (10X Genomics platform). TCR libraries were then sequenced on MiSeq or Nextseq (Illumina).

### TCR $\alpha\beta$ construct generation and screening

TCR $\alpha\beta$  were constructed from synthetic DNA fragments (IDT and Swift Biosciences). Some TCRs were made as retroviral vectors as described previously (Nesterenko et al., 2021). Some constructs were built into the small pMAX vector (Lonza) designed for

transfection-based expression. TCRs were infected into the Jurkat cell line using centrifugation at 1350G for 90 min at 30C with 5  $\mu$ g/mL of polybrene (Sigma-Aldrich). DNA minipreps were prepared using the QIAprep miniprep kit (Qiagen) and concentration was routinely higher than 200 ng/ $\mu$ L. Cells were transfected with 2  $\mu$ L of DNA, dissolved in water, using the Lonza 4D Nucleofactor (Lonza) in 20  $\mu$ L transfection media from the SE cell Line kit S (Lonza). Lonza pre-installed electroporation protocol for Jurkat clone E6.1 was then used. Cells were rested for 10 min and 80  $\mu$ L of warm R10 media was added. Then total of 100  $\mu$ L was transferred to a 24 well plate with 400  $\mu$ L of warm R10 in each well. Cells were then incubated for 12 h and afterwards they were used for functional assays over the course of three days.

### Stimulation of Jurkat

Jurkat cells were plated in 100  $\mu$ L of R10 media in 96 well U bottom plate. K562 cells expressing HLA-A\*02:01 were then added in 100  $\mu$ L of R10 with 20  $\mu$ g/mL of peptide. Cells were then incubated at 37C, 5% CO<sub>2</sub>. zsGreen (GFP) fluorescence was then measured by FACS analysis. For transfection experiments cells were gated on light scatter, CD8<sup>+</sup>/murine TCR $\beta$ <sup>+</sup>.

### PBMC engineering via retrovirus

Retrovirus was produced as described previously (Nesterenko et al., 2021). PBMCs were activated with CD3/CD28 beads (Thermo Fisher) in 24 well plates at 1:1 ratio. After 3 days, TCR construct or empty construct NGFR control retrovirus was added to the cells with 5  $\mu$ g/mL of polybrene (Sigma-Aldrich). Cells were centrifuged at 1350G for 90 min at 30C. After transduction, 1 mL from each well was removed and fresh media with 2X cytokines was added. On the next day, infection was repeated, and the following day cells were washed. Cells were then cultured for two more days, at which point the CD3/CD28 beads were magnetically removed. At this stage, cells were expanded further and used for downstream assays. Transduction was always confirmed by FACS quantification of secondary transduction marker NGFR, and TCR surface expression was ensured by staining for the murine TCR $\beta$  constant region. Our TCR constructs use mouse constant regions to decrease mis-pairing with endogenous TCRs in PBMCs and allow surface TCR staining.

### Cytotoxicity analysis

K562 target cell lines were co-cultured with TCR engineered PBMCs at a 2:1 effector to target ratio, in supplemented AIM V media without cytokines, with 1  $\mu$ g/mL of CD28/CD49d antibodies (BD). For these experiments, we used K562 target cell line that stably expressed RdRp as well as HLA-A\*02:01. The RdRp negative cell line was used as a control for the assay. The IncuCyte system (Sartorius) was used to quantify GFP surface. Because only the K562 target cells expressed GFP, loss of GFP was interpreted as decrease in the number of live cells. 48 h after addition of effectors to targets, 50  $\mu$ L of supernatant was collected for IFN $\gamma$  ELISA analysis as described previously (Nesterenko et al., 2021) using the OptEIA kit for IFN $\gamma$  detection (BD Biosciences).

### Antibodies

NGFR-PECy7 (Biolegend), murine TCR $\beta$ -APC (Biolegend), CD3-APCCy7 (Thermo Fisher), CD8a-PE (Thermo Fisher), CD4-PECy7 (Biolegend), IFN $\gamma$ -APC (Biolegend), TNF $\alpha$ -FITC (Biolegend), HLA-A2-APC (Thermo Fisher), anti-Strep-tag II (Abcam), secondary goat anti-rabbit IgG HRP (Bio-Rad).

### Protein conservation analysis

Coronavirus protein sequences were collected from NCBI Virus (Hatcher et al., 2017). RefSeq assembly accession numbers as follows: SARS-CoV-2 (GCF\_009858895.2), SARS-CoV-1 (GCF\_000864885.1), OC43 (GCF\_003972325.1), NL63 (GCF\_000853865.1), MERS (GCF\_000901155.1), HKU1 (GCF\_000858765.1), 229E (GCF\_000853505.1). For missing protein accessions, we used BLAST (Altschul et al., 1990) to find the sequence most similar to the respective SARS-CoV-2 protein sequence. We performed multiple sequence alignment and calculated the percent identity matrix using the MUSCLE algorithm (Madeira et al., 2019).

### Lollipop plot generation

SARS-CoV-2 amino acid sequence variations representing 893,589 GISAID (Table S4) sequences were downloaded from CoV-Glue, an online web application for analysis of SARS-CoV-2 virus genome sequences, on 05-01-2021 (Shu and McCauley, 2017; Singer et al., 2020). The sequence of Wuhan-Hu-1 (NCBI, NC\_045512.2) was used as a reference sequence for numbering, nucleotide location, and amino acid variations. CoV-GLUE excludes certain GISAID sequences; information about the total number of sequences retrieved from GISAID and the subset of sequences that passed CoV-GLUE exclusion criteria can be found here (<http://cov-glue.cvr.gla.ac.uk/>). Up-to-date information on SARS-CoV-2 proteins and protein domains was queried from UniProt (<https://www.uniprot.org/>). Data were visualized using the Boutros Plotting Package (v6.0.3) for R (P'ng et al., 2019).

### Comparison of TCRs to publicly available data

The SARS-CoV-2 specific TCR $\beta$  dataset (also known as ImmuneCODE Multiplexed Identification of T cell Receptor Antigen specificity [MIRA]) was downloaded from: <https://clients.adaptivebiotech.com/pub/covid-2020>. GLIPH2 analysis identifies antigen specificity groups based on enrichment of local motifs or global patterns differing by one amino acid in the TCR $\beta$  CDR3 amino acid sequences (Huang et al., 2020). GLIPH2 analysis was performed on the combined set of RdRp specific CoVTCRs and SARS-CoV-2



antigen specific TCRs from ImmuneCODE MIRA dataset (Nolan et al., 2020). TCRs from CD8 T cell experiments (minigene and class I peptide) were included and filtered for productive TCR $\beta$ s. We filtered for GLIPH groups with V gene bias ( $p < 0.01$ ) that contain both CoVTCRs and MIRA TCRs. We mapped the identity of the open reading frame (ORF) targeted by each MIRA TCR and counted the number of MIRA TCRs per ORF for each GLIPH group.

### QUANTIFICATION AND STATISTICAL ANALYSIS

FlowJo was used to analyze flow cytometry data and GraphPad Prism was used to generate plots and statistical analyses. Error bars represent standard deviation. Student's T test was used to compare the groups  $**p > 0.01$ ,  $***p > 0.001$ ,  $p > 0.0001$ . Protein conservation was visualized using the Boutros Plotting Package (v6.0.0) for R (Ping et al., 2019). Epitope homologs were visualized with Clustal Omega (<https://www.ebi.ac.uk/Tools/msa/clustalo/>).